Maximum Thrust Nozzles for Gas Particle Flows

ARNOLD A. ELSBERND*
Kirtland Air Force Base, N. Mex.

AND

JOE D. HOFFMAN†
Purdue University, West Lafayette, Ind.

An optimization analysis is presented for the design of maximum thrust nozzles which contain liquid or solid particles in the flowfield. A design procedure was developed wherein an assumed nozzle contour is analyzed to determine if it is a maximum thrust nozzle, and a relaxation scheme was employed to modify the assumed contour until the maximum thrust contour is obtained. Parametric studies were conducted to illustrate the influence of the particle size, the nozzle inlet angle, the throat radius of curvature, the particle drag and heat-transfer coefficients, the particle to gas mass flow ratio, and the nozzle size.

Nomenclature

A = parameter in the particle drag equation
B = parameter in the system energy equation
C = parameter in the particle energy equation
C_1 = Lagrange multiplier
C_2 = Lagrange multiplier
G = general isoperimetric constraint
h_i = Lagrange multipliers
h_p = enthalpy of the particles
p = pressure
p_o = ambient pressure
T = gas temperature
T_p = particle temperature
u = x direction component of gas velocity
u_p = x direction component of particle velocity
v = y direction component of gas velocity
v_p = y direction component of particle velocity
x = distance along axis of nozzle
y = distance normal to axis of nozzle
y_t = nozzle throat radius
γ = specific heat ratio
η = nozzle contour
ρ = gas density per unit volume of gas
ρ_p = particle density per unit volume of gas
ρ_t = nozzle throat radius of curvature
$( )p$ = particle property
$( )x$ = partial derivative with respect to x
$( )y$ = partial derivative with respect to y
$( )'$ = total derivative with respect to x
d/dx = total derivative with respect to x
$d( )$ = total differential of a variable

Introduction

THE first applications of optimization techniques to the design of maximum thrust nozzles were made by Guderley and Hantsch,[1] Rao[2,3] and Guderley.[4] In these analyses, the problem was formulated to provide maximum thrust across a control surface through the nozzle exit for a constant nozzle length design constraint. Since the optimization functional was expressed along the exit control surface, no dissipative effects in the flowfield could be accounted for, and design constraints not directly related to the exit control surface could not be included.

Guderley and Armitage[5] formulated the optimization problem including the entire flow region affecting the nozzle contour in order to apply design constraints directly related to the nozzle contour. The complexity of the formulation and the numerical solution procedure were greatly increased over the previous formulations.

The Guderley-Armitage approach can be extended to dissipative flows since the entire flow region is considered in the problem formulation. Hoffman and Thompson[6] formulated the problem for gas-particle flows, and Hoffman[7] formulated the problem for nonequilibrium, chemically reacting flows. Further work was performed by Scofield and Hoffman,[8] Humphreys, Thompson and Hoffman,[9] and Johnson, Thompson and Hoffman,[10] to develop numerical schemes and computer programs for the design of maximum thrust nozzles for various flow chemistry models and nozzle geometrical models.

The present work presents the optimization problem formulation and the numerical scheme developed to determine maximum thrust nozzle contours for nozzles with condensed particles in the flowfield. The formulation of the optimization problem follows that presented in Ref. 6. The numerical method employed in the present study is presented in Ref. 11. The results of an extensive parametric study are presented to demonstrate the capabilities of the method.

Gas-Particle Flow Analysis

The governing equations for the axisymmetric gas-particle flow analysis are given in Ref. 12. Those equations are the gas continuity equation, two system momentum equations, a system energy equation, a particle continuity equation, two particle momentum equations, and a particle energy equation. The preceding equations are a set of eight partial differential equations for the eight properties u, v, p, ρ, u_p, v_p, h_p, and ρ_p. This system of equations is hyperbolic, and thus can be solved by applying the method of characteristics. An existing gas-particle flowfield analysis program developed by Kliegel and Nickerson[13] was adapted to provide the evaluation of the flowfield.

The system of characteristic equations provides seven compatibility equations along four distinct characteristic directions, and thus cannot be used alone to solve for the eight dependent variables. This deficiency has been explained by Sauerwein and

Presented as Paper 72-1189 at the AIAA/SAE 8th Joint Propulsion Specialists Conference, New Orleans, La., November 29–December 1, 1972; submitted February 16, 1973; revision received October 5, 1973. This work was sponsored by the Air Force Aero Propulsion Laboratory (RJT), Wright-Patterson Air Force Base, Ohio, under Contract F33615-57-C-1068. The program monitor was Capt. G. J. Jungwirth.

Index categories: Nozzle and Channel Flow; Solid and Hybrid Rocket Engines.

* Lt. Colonel, United States Air Force, Air Force Weapons Laboratory.

† Professor of Mechanical Engineering. Member AIAA.

Fendell[14] as arising due to the assumption that particles do not contribute to the pressure. This results in only one distinct characteristic for the particle governing equations, the particle streamline. However, the particle density term in the particle continuity equation is also dependent on the divergence of streamlines. The absence of a pressure term in the particle governing equations precludes inclusion of the divergence effect in the characteristic equations.

The particle stream function is introduced to resolve the deficiency. Since the total amount of particles passing between the centerline and a given particle streamline must remain constant and the distribution of particles passing the initial-value line can be determined, a numerical accounting technique is employed to determine particle density at each point in the flowfield. With the particle density determined, the remaining seven variables can be determined by application of the seven compatability equations.

The present optimization analysis is concerned only with the supersonic portion of the nozzle contour. Thus, an initial-value line along which all flow properties are known must be specified downstream of the nozzle throat in the supersonic flow region. The transonic analysis employed in the present study is that developed in Ref. 13.

The Optimization Problem

The flowfield model for the optimization analysis is presented in Fig. 1. Only changes in the nozzle wall contour between points A and C in the supersonic region are considered. The contours of the nozzle inlet and throat region are assumed to be fixed. The boundary of the optimization problem consists of three line segments. The nozzle wall, AC, defines the first. Since the nozzle contour upstream of point A is fixed, the flowfield upstream of a right-running Mach line attached at point A is independent of the nozzle contour downstream of point A. Thus, the boundary AB is chosen along a right-running Mach line. The third line segment, BC, closes the region and intersects the nozzle contour at the nozzle lip, point C. No other restrictions are made on line BC in the formulation of the problem. However, line BC is represented as a left-running Mach line in Fig. 1, because the solution of the variational problem shows that BC is a left-running Mach line.

The particles flowing through the nozzle do not follow the wall contour, and there is a region near the wall which contains only gas. The limiting particle streamline is represented in Fig. 1 by the line DE. By definition, the nozzle is not optimum if the limiting particle streamline impinges on the nozzle wall. In cases where the maximum thrust solution results in particle impingement, it is necessary to change the inlet and throat region geometry sufficiently to provide the necessary separation.

The functional which is to be maximized by the calculus of variations is (see Ref. 6)

$$I = \int_A^C [(p-p_o)\eta\eta' + C_1 G + C_2(x)\eta\rho(u\eta' - v)]\,dx + \iint_{ABC} \sum_{i=1}^{8} h_i(x,y)L_i(x,y)\,dy\,dx \qquad (1)$$

where $y = \eta(x)$ is the desired maximum thrust contour. The first term of the line integral is the thrust term. The second term is the general isoperimetric constraint $G(\eta, \dot{\eta}, p)$ and its associated Lagrange multiplier C_1. The third term is the constraint which forces the wall to be a gas streamline, and its associated Lagrange multiplier $C_2(x)$. The area integral constraint contains the eight governing equations $L_i(x,y)$ and their associated Lagrange multipliers $h_i(x,y)$.

The calculus of varitions[15] provides a set of conditions which must be satisfied to maximize a functional. The necessary conditions are the Euler equations applicable in the region ABC, the transversality conditions applicable along the boundaries AB, BC, and CA, the corner conditions applicable at corners formed by the intersection of two boundary line segments, and the Erdmann-Weierstrass condition applicable to corner lines in region ABC. In a supersonic nozzle, physical considerations rule out the class of solutions which include corner lines in region ABC; thus the Erdmann-Weierstrass condition was not employed in this formulation, and the first three conditions are considered sufficient.

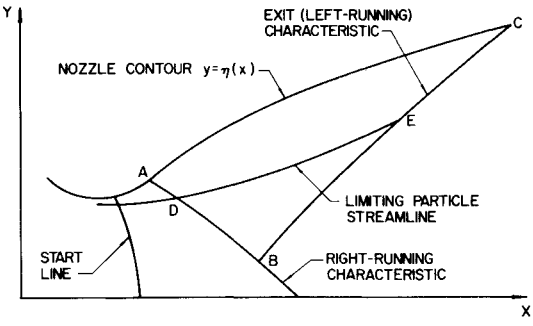

Fig. 1 Gas-particle optimization model.

The Euler equations are eight partial differential equations, which can be employed to evaluate the eight unknown Lagrange multipliers h_1 through h_8. Application of the method of characteristics results in a set of seven compatibility equations applicable along four distinct characteristic directions. The Euler equations and the compatibility equations are presented in Ref. 6.

Since there are eight unknown Lagrange multipliers, h_1 through h_8, and only seven compatability conditions, there is a deficiency of one compatibility equation. The multipliers h_6 and h_7 cannot be evaluated, since derivatives of both appear only in a single compatibility equation. Either h_6 or h_7 must be obtained by another method in order to permit the solution for the other. In this analysis, both were obtained by using a fixed grid finite-difference approximation of the two Euler equations involving h_6 and h_7.

The two Euler equations which contain partial derivatives of h_6 and h_7 are[11]

$$-[u_p(h_6)_x + v_p(h_6)_y] + h_6(u_p)_x + h_7(v_p)_x + h_8(h_p)_x - y(h_5)_x = A\{h_2 - 2h_4(\gamma-1)(u-u_p) - h_6\} - h_6(v_p/y) - [u_p(h_7)_x + v_p(h_7)_y] + h_6(u_p)_y + h_7(v_p)_y + h_8(h_p)_y - \qquad (2)$$

$$y(h_5)_y = A\{h_3 - 2h_4(\gamma-1)(v-v_p) - h_7\} - h_7(v_p/y) \qquad (3)$$

These equations can be solved for the total derivatives of h_6 and h_7 along the particle streamline if all of the remaining partial derivatives can be evaluated numerically. To solve for the partial derivative $(u_p)_x$, the particle x-momentum equation and the definition of the total derivative of u_p are employed.

$$u_p(u_p)_x + v_p(u_p)_y = A(u-u_p) \qquad (4)$$

$$du_p = (u_p)_x\,dx + (u_p)_y\,dy \qquad (5)$$

Equations (4) and (5) are combined to yield

$$(u_p)_x = \frac{A(u-u_p)\,dy - v_p\,du_p}{u_p\,dy - v_p\,dx} \qquad (6)$$

Along the particle streamline, $(u_p)_x$ is indeterminate. However, $(u_p)_x$ can be evaluated numerically along a right- or left-running Mach line in the region of interest, and the resulting numerical value can be employed in Eq. (2).

In a similar manner

$$(v_p)_x = \frac{A(v-v_p)\,dy - v_p\,dv_p}{u_p\,dy - v_p\,dx} \qquad (7)$$

$$(h_p)_x = \frac{\frac{2}{3}AC(T-T_p)\,dy - v_p\,dh_p}{u_p\,dy - v_p\,dx} \qquad (8)$$

$$(u_p)_y = -\frac{A(u-u_p)\,dx - u_p\,du_p}{u_p\,dy - v_p\,dx} \qquad (9)$$

$$(v_p)_y = -\frac{A(v-v_p)\,dx - u_p\,dv_p}{u_p\,dy - v_p\,dx} \qquad (10)$$

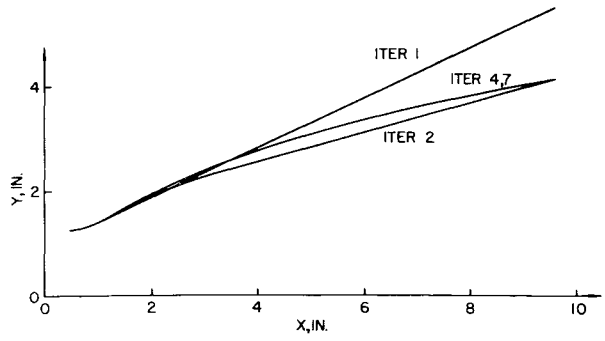

Fig. 2 Nozzle contour behavior.

$$(h_p)_y = -\frac{\frac{2}{3}AC(T-T_p)\,dx - u_p\,dh_p}{u_p\,dy - v_p\,dx} \tag{11}$$

A third Euler equation is given by[11]

$$y\{u_p(h_5)_x + v_p(h_5)_y\} = A\{h_2(u-u_p) + h_3(v-v_p) - h_4 B\} \tag{12}$$

Combining Eq. (12) and the definition of the total derivative of h_5, the following expressions are obtained:

$$(h_5)_x = \frac{A[h_2(u-u_p) + h_3(v-v_p) - h_4 B]\,dy - yv_p\,dh_5}{yu_p\,dy - yv_p\,dx} \tag{13}$$

$$(h_5)_y = \frac{A[h_2(u-u_p) + h_3(v-v_p) - h_4 B]\,dx - yu_p\,dh_5}{yu_p\,dy - yv_p\,dx} \tag{14}$$

The partial derivatives expressed by Eqs. (6–11, 13, and 14), can be evaluated numerically. The results can be substituted into Eqs. (2) and (3) to yield

$$u_p\,dh_6 = [-h_6(u_p)_x - h_7(v_p)_x - h_8(h_p)_x + y(h_5)_x + A\{h_2 - 2h_4(\gamma-1)(u-u_p) - h_6\} - h_6(v_p/y)]\,dx \tag{15}$$

$$u_p\,dh_7 = [-h_6(u_p)_y - h_7(v_p)_y - h_8(h_p)_y + v(h_5)_y + A\{h_3 - 2h_4(\gamma-1)(v-v_p) - h_7\} - h_7(v_p/y)]\,dx \tag{16}$$

The set of six compatibility equations (the original seven equations less the one containing derivatives of h_6 and h_7) and the two Eqs. (15) and (16) can be solved numerically for the Lagrange multipliers h_1 through h_8. Since the expressions for $(h_5)_x$ and $(h_5)_y$ contain the other Lagrange multipliers, the aforementioned set of equations must be solved iteratively.

Application of the calculus of variations also yields two corner conditions at point C, from which the constant multiplier C_1 can be evaluated, and from which an initial value of the multiplier $C_2(x)$ can be determined. Also obtained from the variational solution are a set of seven transversality equations along line BC, and two tranversality equations along line CA.

Those corner conditions and transversality equations are presented in Ref. 6, where a method for employing those equations to evaluate the Lagrange multipliers throughout region ABC is presented. In that procedure, only eight of the nine available transversality equations are required as boundary conditions for evaluating the eight Lagrange multipliers. Thus, one of the transversality equations is not employed in the evaluation of the Lagrange multipliers. That equation is

$$uh_3 - vh_2 + v\eta + uC_1 G_p = 0 \tag{17}$$

which holds along line CA. However, that equation must still be satisfied for a maximum thrust nozzle. Equation (17) is treated as an error function which is used in a relaxation method to obtain the desired maximum thrust nozzle contour.

Relaxation Method

The solution procedure consists of assuming a potential optimum nozzle contour, performing a flowfield analysis, computing the Lagrange multipliers, evaluating the error condition given by Eq. (17), and modifying the nozzle contour appropriately. This procedure is repeated using the modified nozzle contour until the error condition is satisfied to some level of accuracy.

For the initial assumed contour, Eq. (17) will not, in general, be satisfied. An error condition is defined by rewriting Eq. (17) as follows

$$E = \tan^{-1}(\eta') - \tan^{-1}\left\{\frac{h_3 + C_1 G_p}{h_2 - \eta}\right\} \tag{18}$$

By assuming that the remaining variables do not change appreciably with small changes in the wall slope η', the error condition may be relaxed by calculating a new slope so that E will be zero. This new slope is given by

$$\eta' = (h_3 + C_1 G_p)/(h_2 - \eta) \tag{19}$$

A simple integration is performed to determine the relaxed nozzle contour. Thus

$$\eta(x) = \eta(x_A) + \int_{x_A}^{x} \eta'(x)\,dx \tag{20}$$

Since the other variables do change when η' is changed, the relaxation is not exact, and the entire procedure must be iterated to convergence.

A computer program, written in FORTRAN IV for the CDC 6500 computer, was developed based on the analysis and the numerical methods presented herein. This computer program was designed to permit either the analysis of a given nozzle or the design of a maximum thrust nozzle subject to some geometric design constraint. A program description and several sample cases are presented in Ref. 16.

Figures 2 and 3 illustrate the behavior of the optimization scheme for a sample case. The sample case consists of the design of a fixed length nozzle with a length of 9.6 in., a throat radius of 1.2 in., a throat radius of curvature of 2.4 in., and an inlet cone angle of 30°. The initial estimate of the maximum thrust contour is a 25° conical nozzle. Twelve points were specified on the initial-value line. Aluminum oxide particles 4 μ in diameter with a mass flow rate equal to 40% of the gas mass flow rate were considered. The gas properties are specified as $\gamma = 1.28$, molecular weight = 17.76, chamber pressure = 500 psia, chamber temperature = 6500°R, and the ambient pressure is 3 psia. The convergence criterion for the error condition, Eq. (18), was that the wall slope change between successive iterations must be less than 0.05° at each point along the nozzle contour. The operating conditions of this sample case are the nominal conditions of the parametric study presented in the next section.

Seven iterations were required to attain convergence. The initial, second, fourth, and final nozzle contours are shown in

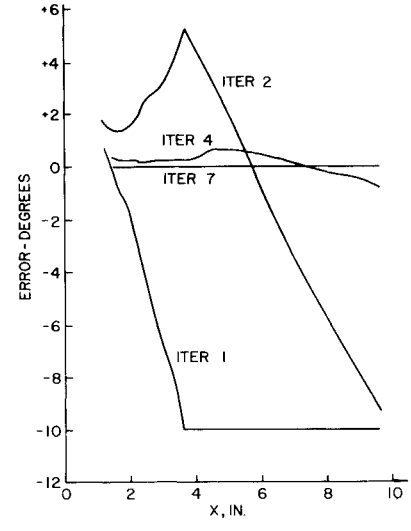

Fig. 3 Error function behavior.

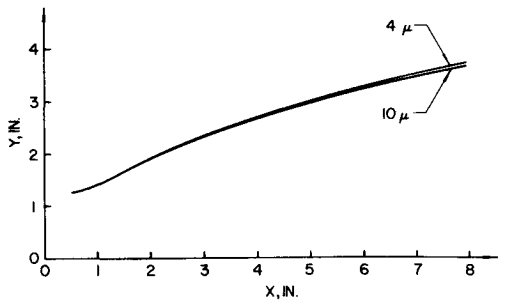

Fig. 4 Effect of particle size on final contour.

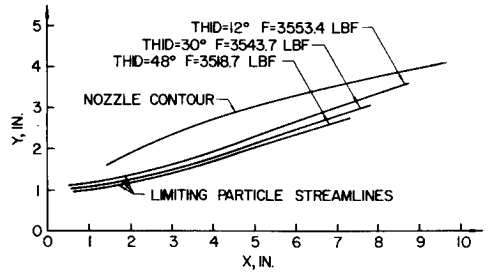

Fig. 6 Inlet angle effects.

Fig. 2. The fourth and final contours are almost identical, indicating that a larger convergence tolerance could have been used. The corresponding error values from Eq. (18) are presented in Fig. 3. The initial contour estimate of a conical nozzle resulted in large error values for the first iteration. However, the change in wall angle at any point along the nozzle contour was limited to a maximum of 10°. The error values for the second iteration show that the initial error was overcorrected near the inlet. The error values for the fourth iteration show a marked decrease in size, and by the seventh iteration, the error values are less than 0.05° at all points. This solution required approximately 40 sec of computing time per iteration on a CDC 6500 computer. Computing time scales approximately as the square of the number of points on the initial-value line.

Parametric Studies

In this section, the results of parametric studies conducted to demonstrate the capabilities of the method are presented. The nominal operating conditions for the parametric study are those presented for the sample case in the last section. Only those parameters which have been changed are discussed here. The first study considered the effect of particle size in an 8-in. long nozzle. Particle sizes of 4, 6, 8, and 10 μ were considered. In all cases, the ratio of the particle to gas mass flow rate was 0.4. The number of initial-value line points, which affects the mesh size throughout the nozzle, was 20. The final contours are shown in Fig. 4. The optimized contours are almost identical. Thus, it appears that any size particle can be used in the design process with very little change in the nozzle contour.

An analysis of off-design operation was made to determine the effect of particle size mismatch. The contours used in the off-design study are the final contours just mentioned. Each contour was analyzed with all of the particle sizes considered. The results of the off-design studies are presented in Table 1. The values along the upper left to lower right diagonal are the on-design results.

Each optimum nozzle contour yields essentially the same thrust regardless of the particle size, within the accuracy of the numerical scheme. Thus, the thrust generated by the optimum

Table 1 Off-design particle size analysis

Particle size used in analysis	Thrust Particle size used in design			
	4 μ	6 μ	8 μ	10 μ
4 μ	3516.2	3516.3	3515.6	3515.9
6 μ	3507.4	3509.3	3508.3	3508.5
8 μ	3503.1	3504.8	3504.3	3504.4
10 μ	3497.0	3501.4	3498.6	3499.2

nozzle contour depends only on the particle size in the actual flow, and not on the particle size employed in the design itself, for the range of particle sizes considered in this study.

A study of the effects of the particle to gas mass flow rate ratio WPWGT was conducted for values of that ratio of 0.1, 0.4, 0.7, and 1.0. The particle size was 4 μ and the number of initial-value line points was 12. The results, shown in Fig. 5, indicate that larger ratios of particle to gas mass flow rate require more expansion to maximize the thrust. This result is due to a combination of drag and heat-transfer effects. The increased transfer of energy between the particles and the gas also results in increased thrust. This study did not consider changes in the combustion properties due to changes in composition.

Values of the nozzle inlet cone angle THID of 12°, 30° and 48° were studied. It was found that the optimum nozzle contour was essentially the same for all three inlet angles. However, the limiting particle streamlines were altered considerably, as shown in Fig. 6. The thrust increased with decreasing nozzle inlet angle, since the particles occupied greater portions of the nozzle, permitting more effective energy transfer. This indicates that the nozzle inlet contour should be designed to bring the limiting particle streamline near the end of the nozzle contour while still avoiding impingement.

Studies were conducted to determine the effect of inaccuracies in the empirical drag and heat-transfer coefficients used in the analysis. Figure 7 presents the results obtained when the drag coefficient C_D was changed by factors of 3 and $\frac{1}{3}$ relative to the standard case, which consists of the default values supplied with the original analysis program.[13] The optimized nozzle contours

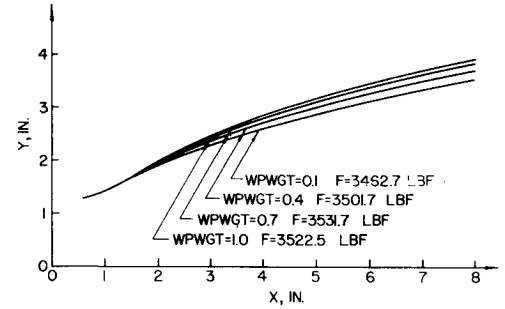

Fig. 5 Effect of particle mass to gas mass ratio.

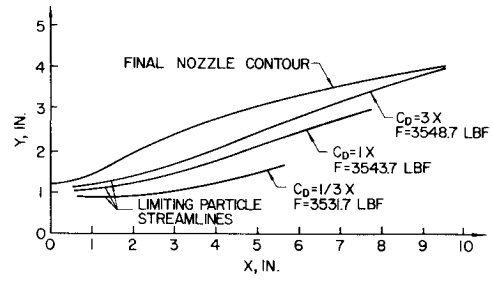

Fig. 7 Effect of drag coefficient variation.

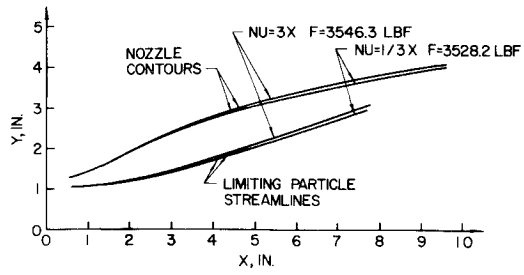

Fig. 8 Effect of heat-transfer coefficient variation.

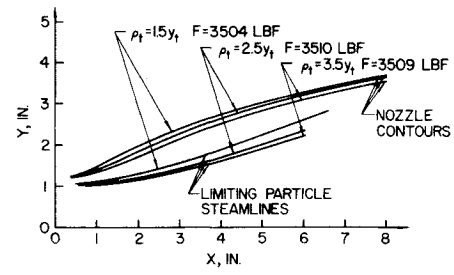

Fig. 9 Effect of throat radius of curvature.

were virtually identical for all three cases. Thus, large variations in drag coefficient appear to have an insignificant effect on the maximum thrust contour. However, the limiting particle streamline was affected substantially, and the larger drag coefficients resulted in greater thrust.

Figure 8 presents the results obtained by varying the heat-transfer coefficient (in terms of the Nusselt number Nu) by factors of 3 and $\frac{1}{3}$. The larger heat-transfer coefficient resulted in a larger value of thrust and a slightly greater nozzle expansion ratio. A ninefold increase in the heat-transfer coefficient increased the thrust 0.5%. Particle impingement was not a problem since the limiting particle streamline moved outward by approximately the same distance as the nozzle contour moved outward. Hence, large variations in the heat-transfer coefficient appear to have a minor effect on the maximum thrust contour.

The effect of the throat radius of curvature ratio $RRT = \rho_t/y_t$ was investigated for values of RRT equal to 1.5, 2.5, and 3.5, for an 8-in. long nozzle. As illustrated in Fig. 9, the thrust values are approximately equal, although the nozzle contours and expansion ratios vary. The nozzle contours are very similar, however, if they are translated in the axial direction a sufficient distance to compensate for the variation in throat length. The limiting particle streamline was also affected by the change in the throat radius of curvature. With larger values of RRT, the curvature of the wall at the throat region is more gradual, permitting the particles to accelerate more in the axial direction prior to being subjected to vertical drag forces. This effect results in a greater separation between the nozzle wall and the limiting particle streamline. This result indicates that it may be advantageous to use a larger throat radius of curvature, since thrust is not lost, particle impingement with the wall is avoided, and there is a possibility that the nozzle weight could be reduced, due to the smaller expansion ratio.

Figure 10 illustrates the effects of nozzle size. The reference nozzle ($1X$) is a 4.8-in. long nozzle with a throat radius of 0.6 in., an inlet angle of 45°, and a throat radius of curvature of three throat radii. Additional cases were studied for nozzle sizes two times ($2X$), four times ($4X$), and eight times ($8X$) the size of the reference nozzle. As illustrated in Fig. 10, the optimum nozzle contours do not scale, the larger nozzles having a greater expansion ratio. The limiting particle streamline locations show a marked variation as the nozzle size is changed. The thrust for each of the final contours is shown in Table 2. If the thrust scaled directly with nozzle size, the thrust would increase as the square of the nozzle scale factor. The results show that the thrust increase is slightly higher than direct scaling would predict. For the $8X$ case, the thrust increase over direct scalings is 1.2%.

Table 2 Thrust evaluation for nozzle scaling

Nozzle size	Thrust	Thrust ratio
$1X$	883.4	1.000
$2X$	3543.1	4.011
$4X$	14223.1	16.100
$8X$	57208.4	64.759

For purposes of comparison with conical nozzles, consider the nozzle designed for 4 μ diameter particles in the particle size study. That nozzle had a throat radius of 1.2 in., a throat radius of curvature of 2.4 in., and a length of 8 in. Three conical nozzles are compared with that maximum thrust nozzle, which had a thrust of 3516.2 lbf. These are a 15° conical nozzle of the same length, a 15° conical nozzle of the same area ratio (which required a length of 9.711 in.), and a conical nozzle having the same length and area ratio (which required a cone angle of 18.34°). The results are tabulated in Table 3.

Table 3 Conical nozzle comparison

Angle	Length	Thrust	ΔF, %
15°	8.000	3487.92	−0.80
15°	9.711	3532.96	+0.48
18.34°	8.000	3495.24	−0.60

As shown in Table 3, the thrust gain of the maximum thrust nozzle relative to the 15° and 18.34° conical nozzles of the same length as the maximum thrust nozzle is 0.80% and 0.60%, respectively. The 15° conical nozzle of the same area ratio yielded 0.48% more thrust than the maximum thrust nozzle, but it was 21.4% longer. A maximum thrust nozzle 9.711 in. long would develop more thrust than the 15° conical nozzle of that length. This difference between the performance of maximum thrust nozzles and conical nozzles becomes more pronounced as the design length is decreased.

Conclusions

The maximum thrust nozzle design problem for axisymmetric gas-particle flows has been formulated and solved. A computer program was developed to implement the design procedure. Several parametric studies were conducted to determine the effect of various parameters on the nozzle shape, the limiting particle streamline location, and the thrust of optimum nozzles. Several conclusions based on those studies can be drawn:

1) The effect of particle size on the maximum thrust nozzle contour is insignificant.

2) The ratio of the particle to gas mass flow rate has a

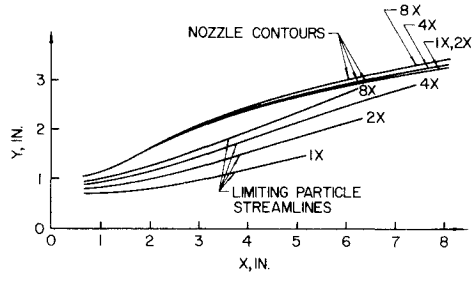

Fig. 10 Effect of scaling.

significant effect on both the maximum thrust nozzle contour and the thrust. Higher concentrations of particles require a greater expansion ratio to develop the maximum thrust and develop greater thrust.

3) Variation of the inlet angle to the nozzle throat does not appreciably affect the final nozzle contour, but does affect the position of the limiting particle streamline and the thrust. Smaller inlet angles result in particles occupying a greater portion of the nozzle and yield a greater thrust.

4) Increasing the value of the drag coefficient does not appreciably affect the nozzle contour, but increases the portion of the nozzle which contains particles, and increases the thrust.

5) Increasing the heat-transfer coefficient increases the expansion ratio of the final nozzle contour, increases the portion of the nozzle which contains particles, and increases the thrust.

6) Increasing the throat radius of curvature decreases the nozzle exit diameter but does not affect the thrust significantly. An increased throat radius of curvature results in greater separation between the limiting particle streamline and the nozzle contour.

7) Increasing the nozzle size changes the nozzle contour slightly, and results in significant thrust increases if the nozzle scaling factor is large and the original nozzle is small.

References

[1] Guderley, G. and Hantsch, E., "Beste Formen für Achsensymmetrische Überschallschubdusen," *Zeitschrift für Flugwissenschaften*, Vol. 3, 1955, pp. 305–313.

[2] Rao, G. V. R., "Exhaust Nozzle Contour for Optimum Thrust," *Jet Propulsion*, Vol. 28, 1958, pp. 377–382.

[3] Rao, G. V. R., "Spike Nozzle Contour for Optimum Thrust," *Ballistic Missile and Space Technology*, Vol. 2, edited by C. W. Morrow, Pergamon Press, New York, 1961, pp. 92–101.

[4] Guderley, G., "On Rao's Method for the Computation of Exhaust Nozzles," *Zeitschrift für Flugwissenschaften*, Vol. 7, 1959, pp. 345–350.

[5] Guderley, K. G. and Armitage, J. V., "General Approach to Optimum Rocket Nozzles," *Theory of Optimum Aerodynamic Shapes*, edited by A. Miele, Academic Press, New York, 1965, Chap. 11, pp. 161–183.

[6] Hoffman, J. D. and Thompson, H. D., "A General Method for Determining Optimum Thrust Nozzle Contours for Gas-Particle Flows," *AIAA Journal*, Vol. 5, No. 10, Oct. 1967, pp. 1886–1887.

[7] Hoffman, J. D., "A General Method for Determining Optimum Thrust Nozzle Contours for Chemically Reacting Gas Flows," *AIAA Journal*, Vol. 5, No. 4, April 1967, pp. 670–676.

[8] Scofield, M. P. and Hoffman, J. D., "Maximum Thrust Nozzles for Nonequilibrium Simple Dissociating Gas Flows," *AIAA Journal*, Vol. 9, No. 9, Sept. 1971, pp. 1824–1832.

[9] Humphreys, R. P., Thompson, H. D., and Hoffman, J. D., "Design of Maximum Thrust Plug Nozzles for Fixed Inlet Geometry," *AIAA Journal*, Vol. 9, No. 8, Aug. 1971, pp. 1581–1587.

[10] Johnson, G. R., Thompson, H. D., and Hoffman, J. D., "Design of Maximum Thrust Plug Nozzles with Variable Inlet Geometry," Vols. 1 and 2, AFAPL-TR-70-75, Oct. 1970, Air Force Aero Propulsion Lab., Wright-Patterson Air Force Base, Ohio.

[11] Elsbernd, A. A. and Hoffman, J. D., "Design of Maximum Thrust Axisymmetric Nozzles with Two-Phase Flow, Vol. I, Theoretical Development and Results," AFAPL-TR-71-52, June 1971 Air Force Aero Propulsion Lab., Wright-Patterson Air Force Base, Ohio.

[12] Kliegel, J. R. and Nickerson, G. R., "Flow of Gas-Particle Mixtures in Axially Symmetric Nozzles," *Progress in Astronautics and Rocketry, Vol. 6, Detonation and Two-Phase Flow*, Academic Press, New York, 1962, pp. 173–194.

[13] Kliegel, J. R. and Nickerson, G. R., "Axisymmetric Two-Phase Perfect Gas Performance Program," 02874-6006-R000, April 1967, TRW Systems, Redondo Beach, Calif.

[14] Sauerwein, H. and Fendell, F. E., "Method of Characteristics in Two Phase Flow," *Physics of Fluids*, Vol. 8, Aug. 1966, pp. 1564–1565.

[15] Miele, A., "Generalized Approach to the Calculus of Variations in Two Independent Variables," *Theory of Optimum Aerodynamic Shapes*, Academic Press, New York, 1965, Chap. 4, pp. 57–74.

[16] Elsbernd, A. A. and Hoffman, J. D., "Design of Maximum Thrust Axisymmetric Nozzles with Two-Phase Flow, Vol. II, Computer Program Manual," AFAPL-TR-71-52, June 1971, Air Force Aero Propulsion Lab., Wright-Patterson Air Force Base, Ohio.